A Refined Direct Position Determination Method for Information Fusion in Sensor Networks

Yuan Zhang[1], Guizhou Wu[1], Fucheng Guo[1], Shuqiang Zhang[1]
{zhangyuan@nudt.edu.cn, wuguizhou@nudt.edu.cn, gfcly75@163.com, zsq391221@163.com}
[1]National University of Defense Technology, 109 Deya St, Changsha 410073, China

Abstract. Passive localization using sensor networks often employs direct position determination (DPD), which performs well in low-SNR conditions. To improve the localization spectrum for subsequent multi-source data fusion, this paper proposes a refined DPD method based on maximum eigenvalue trace (MET-DPD). Unlike conventional DPD, which uses only the maximum eigenvalue, MET-DPD exploits eigendecomposition information more thoroughly by constructing a cost function from the ratio of the maximum eigenvalue to the sum of the remaining eigenvalues of the signal covariance matrix. Simulations show that MET-DPD yields a sharper and more accurate spectrum than existing methods, thereby providing higher-quality preprocessed image data for fusion with optical, infrared, and other sensing modalities.

Keywords: direct position determination, sensor networks, localization cost function, eigenvalue decomposition

1 Introduction

Passive localization technology has become a research hotspot in recent years and is widely used in military and civilian fields [1–3], including target reconnaissance, electromagnetic detection, and smart city applications. It enables the detection and localization of emitters such as drones and communication base-stations.

With the performance improvement and increasingly widespread deployment of advanced sensor technology [4, 5], how to efficiently utilize sensor networks to achieve high-precision perception of the surrounding electromagnetic environment has emerged as a current research focus. When electronic devices such as drones or base-stations transmit signals, sensor networks can intercept these signals and estimate the positions through passive location technology.

Currently, mainstream passive localization approaches are divided into two-step methods and direct position determination (DPD) methods. In two-step methods [1, 4], the intermediate localization parameters, such as Direction of Arrival (DOA), Time Difference of Arrival (TDOA), Frequency Difference of Arrival (FDOA) or their varying rate, are first estimated from the intercepted signals. Then, the position is calculated based on these parameters. This approach has a clear physical interpretation and relatively low computational complexity. However, it is inherently suboptimal and less

IIKI 2025, December 18-21, Chengdu, People's Republic of China

DOI 10.4108/eai.18-12-2025.2365303

effective in processing weak signals. The DPD methods [2–4], also known as the one-step methods, process the intercepted signals directly by constructing a localization cost function to estimate the emitter position. By avoiding explicit estimation of intermediate parameters, it represents an optimal estimator and performs better under low signal-to-noise ratio (SNR) conditions. Nevertheless, because it operates directly on the raw intercepted signals, DPD methods entail higher transmission requirements and computational complexity [2, 3].

This paper focuses on direct position determination for three main reasons: the increasing proliferation of electronic devices in modern urban environments leads to weaker signals intercepted by sensor networks [5, 8], necessitating high localization accuracy under low-SNR conditions; advancements in modern mobile communication technologies and high-performance computing networks have significantly reduced transmission and computational costs, making DPD feasible [10]; DPD method can generate a cost function spectrum over the region of interest, which facilitates subsequent multi-source information fusion with optical, infrared, or other image data for enhanced situational awareness [8].

The existing research on multi-station direct position determination primarily aims to improve localization accuracy and reduce processing complexity, including refining the localization cost function [7], optimizing the position search algorithms [7, 9], and enhancing the system workflow [6]. Some studies utilize the signals characteristic information and refine the cost function for accuracy improvement [6, 7]. The above studies focus on independent localization processing and obtaining estimated position of emitters, rather than considering the cost function spectrum image as pre-processing data for further multi-source information fusion in reconnaissance and sensing. Nevertheless, with the development of advanced sensor networks, it is necessary to consider how to integrate data from various types of sensors including optical and infrared ones, which is the main difference between the starting point of this study and existing research.

In this paper, a novel DPD cost function based on Maximum Eigenvalue Trace (MET) is proposed to improve the pre-processed data quality for subsequent multi-source perception information fusion. Section 2 formulates the signal model in sensor networks, while in Section 3, the proposed MET-DPD method is described in detail. Cramér-Rao Lower Bound and simulations are illustrated in Section 4 and Section 5 to prove the effectiveness. Finally, Section 6 concludes this paper.

2 Signal Model

In this section, the signal model is established. The space dimension is denoted as $d = 2$, which can be adapted to 3-D scenario. The emitter is located in unknown position $\boldsymbol{u}_0 = [x_0, y_0]^T$. As shown in Fig.1, there are M spatially separated sensors deployed to passively receive signals transmitted from the emitter $\boldsymbol{u}_0$. The signal is expressed as

$$s(t) = x(t)\exp(j2\pi f_0 t) \tag{1}$$

where j is the imaginary unit with $j^2 = -1$, $x(t)$ denotes the baseband signal and the bandwidth of $x(t)$ is W, f_0 represents the carrier frequency. The position and velocity of the m^{th} sensor are $\boldsymbol{p}_m = [x_m^o, y_m^o]^T$ and $\boldsymbol{v}_m = [\dot{x}_m^o, \dot{y}_m^o]^T$. Assume that signals are transmitted through line-of-sight (LoS)

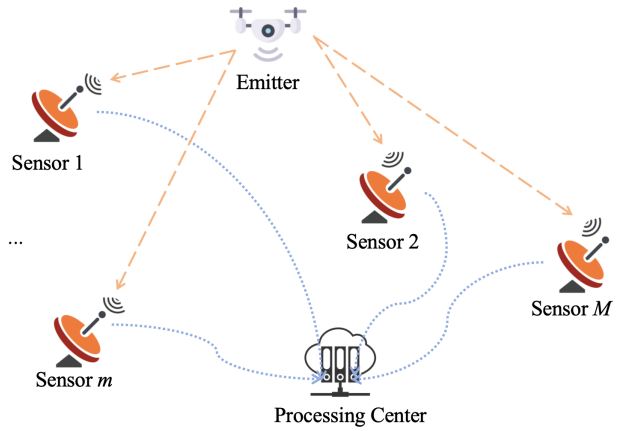

Fig. 1. Schematic Diagram of Localization Scenario

propagation and the multi-path effect can be ignored. The intercepted signals by m^{th} sensor can be represented as

$$r_m(t) = a_m x(t-\tau_m^o)\exp(j2\pi f_m^o t) + \omega_m(t) \tag{2}$$

with the signal attenuation factor a_m. The propagation time τ_m^o and the doppler frequency shift f_m^o are given by

$$\begin{aligned} \tau_m^o &= \frac{\|\boldsymbol{u}_0-\boldsymbol{p}_m\|}{c} \\ f_m^o &= f_0\frac{\boldsymbol{v}_m^T(\boldsymbol{u}_0-\boldsymbol{p}_m)}{c\|\boldsymbol{u}_0-\boldsymbol{p}_m\|} \end{aligned} \tag{3}$$

where c is the propagation speed of signals. $\omega_m(t)$ represents the addictive white Gaussian noise with variance σ_m^2.

The signal in (2) can be reformulated by

$$r_m(t) = b_m r_{1,l}^o(t-\tilde{\tau}_m)\exp(j2\pi\tilde{f}_m t) + w_m(t) \tag{4}$$

with

$$\begin{aligned} \tilde{\tau}_m &= \tau_m^o - \tau_{1,l}^o \\ \tilde{f}_m &= f_m^o - f_{1,l}^o \end{aligned} \tag{5}$$

where r_1^o is the noise-free reference signal received by the 1^{st} sensor, $b_m = a_m/a_1$ is real-valued relative gain between the signal of m^{th} sensor and the reference signal.

It is important to note that the time delay and Doppler shift are not quantities to be estimated, but only work as intrinsic parameters to establish a connection between the intercepted signals and the emitter position.

Sample $r_m(t)$ discretely with sampling frequency f_s, so the uniform time interval is $t_s = 1/f_s$. The sampled signal can be written as $r_m(n) \equiv r_m(t = nt_s), n = 1,2,...,N$. Reformulate the discrete

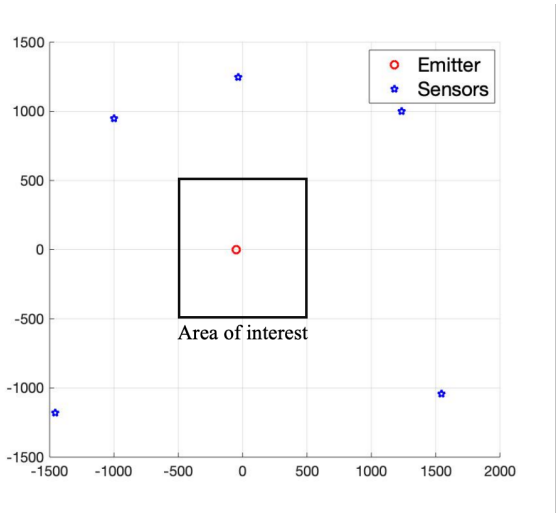

Fig. 2. Simulation Scene

signal as

$$\boldsymbol{r}_m = b_m \boldsymbol{D}_{f_m} \boldsymbol{F}^H \boldsymbol{D}_{\tau_m} \boldsymbol{F} \boldsymbol{r}_1^o + \boldsymbol{w}_m \tag{6}$$

Denote the Doppler frequency shift operator and the time delay operator as

$$\begin{aligned} \boldsymbol{D}_{f_m} &= \mathrm{diag}\left\{\exp[j2\pi \tilde{f}_m (N/2+\boldsymbol{n})]\right\} \\ \boldsymbol{D}_{\tau_m} &= \mathrm{diag}\left\{\exp[-j2\pi fs/N \boldsymbol{n} \tilde{\tau}_m]\right\} \end{aligned} \tag{7}$$

where $\boldsymbol{n} = [-N/2, -N/2+1, ..., N/2-1]^T$ is the index sequence, and the fast Fourier transform (FFT) matrix is $\boldsymbol{F} = \frac{1}{\sqrt{N}} \exp\left\{j2\pi \boldsymbol{n}\boldsymbol{n}^T/N\right\}$.

Define the time-frequency operator of m^{th} sensor in l^{th} interval as

$$\boldsymbol{Q}_m = \boldsymbol{D}_{f_m} \boldsymbol{F}^H \boldsymbol{D}_{\tau_m} \boldsymbol{F} \tag{8}$$

(6) can be reformulated as

$$\boldsymbol{r}_m = b_m \boldsymbol{Q}_m \boldsymbol{r}_1^o + \boldsymbol{w}_m \tag{9}$$

This model is applicable to stationary sensor networks, where relative motion is absent.

3 Refined Direct Position Determination with Maximum Eigenvalue Trace

In this section, a refined direct position determination method based on the maximum eigenvalue and the trace (MET-DPD) is proposed. Compared to the classic DPD based on the maximum eigenvalue, MET-DPD can make fuller use of signal feature information, thus improving processing performance.

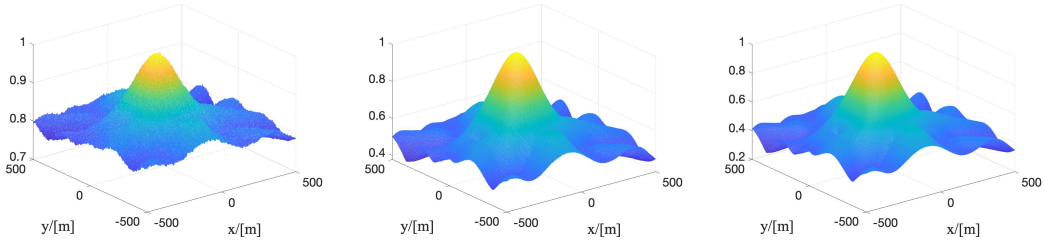

(a) -10dB (b) 0dB (c) 10dB

Fig. 3. Cost Function Spectrum of ME-DPD

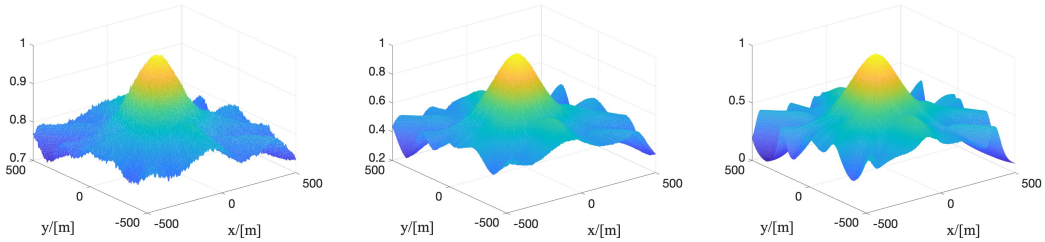

(a) -10dB (b) 0dB (c) 10dB

Fig. 4. Cost Function Spectrum of MME-DPD

The unknown parameter set is defined as

$$\boldsymbol{\theta} = [(\boldsymbol{r}_1^o)^T, \boldsymbol{b}^T, \boldsymbol{u}^T]^T \tag{10}$$

with the relative attenuation factor $\boldsymbol{b} = [b_1, ..., b_M]^T$.

The log likelihood function of intercepted signals by sensor networks is given by

$$\ln P(\boldsymbol{r}|\boldsymbol{\theta}) = c_0 - \frac{1}{2\sigma_n} \sum_{m=1}^{M} ||\boldsymbol{r}_m - b_m \boldsymbol{Q}_m \boldsymbol{r}_1^o||^2 \tag{11}$$

where c_0 is a constant independent of $\boldsymbol{b}$.

The likelihood function in (11) can reach global minimum when $\boldsymbol{u}$ is the true source position. The localization cost function is

$$C(\boldsymbol{\theta}) = \sum_{m=1}^{M} \frac{1}{2\sigma_m} ||\boldsymbol{r}_m - b_m \boldsymbol{Q}_m \boldsymbol{r}_1^o||^2 \tag{12}$$

b_m can be estimated by maximum-likelihood (ML) criterion by setting the partial derivative of (12)

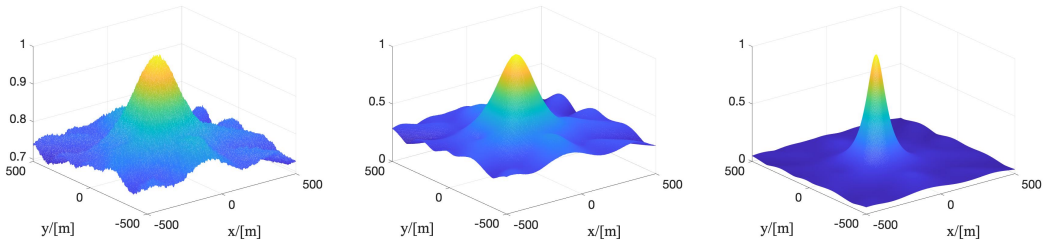

(a) -10dB (b) 0dB (c) 10dB

Fig. 5. Cost Function Spectrum of MET-DPD

as zero [2, 7]

$$\hat{b}_m = \frac{(\boldsymbol{r}_1^o)^H \boldsymbol{Q}_m^H \boldsymbol{r}_m}{\|\boldsymbol{r}_1^o\|^2} \tag{13}$$

Substitute (13) into (12)

$$C(\boldsymbol{u}, \boldsymbol{r}_1^o, \boldsymbol{b}) = \frac{(\boldsymbol{r}_1^o)^H \left(\sum_{m=1}^{M} \frac{1}{2\sigma_m} \boldsymbol{Q}_m^H \boldsymbol{r}_m \boldsymbol{r}_m^H \boldsymbol{Q}_m \right) \boldsymbol{r}_1^o}{\|\boldsymbol{r}_1^o\|^2} \tag{14}$$

$\boldsymbol{r}_1^o / \|\boldsymbol{r}_1^o\|$ is the eigenvector corresponding to the maximum eigenvalue of $\boldsymbol{A}\boldsymbol{X}\boldsymbol{X}^H$ with $\boldsymbol{X} = [\boldsymbol{r}_1, \boldsymbol{Q}_2^H \boldsymbol{r}_2, ..., \boldsymbol{Q}_M^H \boldsymbol{r}_M]$, $\boldsymbol{A} = \text{diag}\{1/\sigma_1, 1/\sigma_2, ..., 1/\sigma_M\}$.

The DPD cost function based on the maximum eigenvalue is denoted as [2, 3]

$$C_{DPD}(\boldsymbol{u}) = \lambda_{max}(\boldsymbol{A}\boldsymbol{X}\boldsymbol{X}^H) \tag{15}$$

where$\lambda_{max}(\cdot)$ is the maximum eigenvalue. Note that the non-zero eigenvalues of $\boldsymbol{X}\boldsymbol{X}^H$ are equal to the non-zero eigenvalues of $\boldsymbol{X}^H\boldsymbol{X}$. The classic cost function can be rewritten as

$$C_{DPD}(\boldsymbol{u}) = \lambda_{max}(\boldsymbol{A}\boldsymbol{X}^H\boldsymbol{X}) \tag{16}$$

The eigenvalue decomposition information is not utilized completely in (16). The physical meaning of the maximum eigenvalue and the trace of $\boldsymbol{A}\boldsymbol{X}^H\boldsymbol{X}$ correspond to the energy of emitter signal and the energy of the intercepted signal respectively. Refine the cost function in (16) as

$$C'_{DPD}(\boldsymbol{u}) = \frac{\lambda_{max}(\boldsymbol{A}\boldsymbol{X}^H\boldsymbol{X})}{\text{tr}(\boldsymbol{A}\boldsymbol{X}^H\boldsymbol{X}) - \lambda_{max}(\boldsymbol{A}\boldsymbol{X}^H\boldsymbol{X})} \tag{17}$$

where $\text{tr}(\cdot)$ represents the matrix trace. The physical meaning of (17) is the ratio of emitter signal and noise, which can better reflect characteristic information of the intercepted signals.

4 Cramér-Rao Lower Bound

The Cramér-Rao Lower Bound (CRLB) provides a theoretical lower limit for the accuracy of unbiased estimation in localization. Define the unknown real-valued parameter vector as $\boldsymbol{\zeta}$, which includes the real part $\mathrm{Re}\{\boldsymbol{r}^o\}$ and imaginary part $\mathrm{Im}\{\boldsymbol{r}^o\}$ of the reference signal, relative gain $\boldsymbol{b} = [b_1, ..., b_M]^T$ and the emitter position $\boldsymbol{u}$.

$$\boldsymbol{\zeta} = [\mathrm{Re}\{\boldsymbol{r}^o\}, \mathrm{Im}\{\boldsymbol{r}^o\}, \boldsymbol{b}, \boldsymbol{u}]^T \tag{18}$$

The Fisher Information Matrix (FIM) of $\boldsymbol{\zeta}$ under the additive white Gaussian noise scenarios is denoted as

$$\boldsymbol{J}_{\boldsymbol{\zeta}} = \begin{bmatrix} \boldsymbol{J}_{\boldsymbol{r}^o\boldsymbol{r}^o} & \boldsymbol{J}_{\boldsymbol{r}^o\boldsymbol{b}} & \boldsymbol{J}_{\boldsymbol{r}^o\boldsymbol{u}} \\ \boldsymbol{J}_{\boldsymbol{b}\boldsymbol{r}^o} & \boldsymbol{J}_{\boldsymbol{b}\boldsymbol{b}} & \boldsymbol{J}_{\boldsymbol{b}\boldsymbol{u}} \\ \boldsymbol{J}_{\boldsymbol{u}\boldsymbol{r}^o} & \boldsymbol{J}_{\boldsymbol{u}\boldsymbol{b}} & \boldsymbol{J}_{\boldsymbol{u}\boldsymbol{u}} \end{bmatrix} \tag{19}$$

where the second-order partial derivatives are

$$[\boldsymbol{J}_{\boldsymbol{\zeta}}]_{ij} = -E\left[\frac{\partial \ln^2 P(\boldsymbol{r}|\boldsymbol{\zeta})}{\partial \boldsymbol{\zeta}_i \partial \boldsymbol{\zeta}_j}\right] \tag{20}$$

For the intercepted signal model in Section 2, there are

$$\begin{aligned} &\boldsymbol{J}_{\boldsymbol{r}^o\boldsymbol{r}^o} = \begin{bmatrix} \boldsymbol{J}_1 & \boldsymbol{0}_N \\ \boldsymbol{0}_N & \boldsymbol{J}_1 \end{bmatrix} \\ &\boldsymbol{J}_{\boldsymbol{r}^o\boldsymbol{b}} = \begin{bmatrix} \mathrm{Re}(\boldsymbol{J}_3) & \mathrm{Im}(\boldsymbol{J}_3) \end{bmatrix}^T \\ &\boldsymbol{J}_{\boldsymbol{r}^o\boldsymbol{u}} = \begin{bmatrix} \mathrm{Re}(\boldsymbol{J}_4) & \mathrm{Im}(\boldsymbol{J}_4) \end{bmatrix}^T \\ &\boldsymbol{J}_{\boldsymbol{b}\boldsymbol{u}} = \mathrm{Re}(\boldsymbol{J}_5),\ \boldsymbol{J}_{\boldsymbol{b}\boldsymbol{b}} = \boldsymbol{J}_2,\ \boldsymbol{J}_{\boldsymbol{u}\boldsymbol{u}} = \boldsymbol{J}_6 \end{aligned} \tag{21}$$

where

$$\begin{aligned} &\boldsymbol{J}_1 = \textstyle\sum \frac{b_m^2}{\sigma_m} \boldsymbol{I}_N, \qquad \boldsymbol{J}_2 = \textstyle\sum \frac{1}{\sigma_m} (\boldsymbol{r}^o)^H \boldsymbol{r}^o \boldsymbol{I}_M \\ &\boldsymbol{J}_3 = \boldsymbol{\sigma} \cdot (\boldsymbol{A}^H \boldsymbol{B}), \quad \boldsymbol{J}_4 = \boldsymbol{\sigma} \cdot (\boldsymbol{A}^H \boldsymbol{C}) \\ &\boldsymbol{J}_5 = \boldsymbol{\sigma} \cdot (\boldsymbol{B}^H \boldsymbol{C}), \quad \boldsymbol{J}_6 = \textstyle\sum \frac{1}{\sigma_m} (\boldsymbol{C}_m^H \boldsymbol{C}_m) \end{aligned} \tag{22}$$

where $\boldsymbol{\sigma}$ is the noise variance vector, $\otimes$ is the Kronecker product, and matrices $\boldsymbol{A}$, $\boldsymbol{B}$, $\boldsymbol{C}$ given by

$$\begin{aligned} &\boldsymbol{\sigma} = [1/\sigma_1, 1/\sigma_2, \cdots, 1/\sigma_M] \\ &\boldsymbol{A} = [b_1 \boldsymbol{Q}_1, b_2 \boldsymbol{Q}_2, \cdots, b_M \boldsymbol{Q}_M]^T \\ &\boldsymbol{B} = \mathrm{diag}\{b_1 \boldsymbol{Q}_1, b_2 \boldsymbol{Q}_2, \cdots, b_M \boldsymbol{Q}_M\} \cdot (\boldsymbol{I}_M \otimes \boldsymbol{r}^o) \\ &\boldsymbol{C} = [\boldsymbol{C}_1, \boldsymbol{C}_2, \cdots, \boldsymbol{C}_M]^T \end{aligned} \tag{23}$$

with

$$\boldsymbol{C}_m = \left[\frac{\partial b_m \boldsymbol{Q}_m \boldsymbol{r}^o}{\partial x}, \frac{\partial b_m \boldsymbol{Q}_m \boldsymbol{r}^o}{\partial y}\right] \tag{24}$$

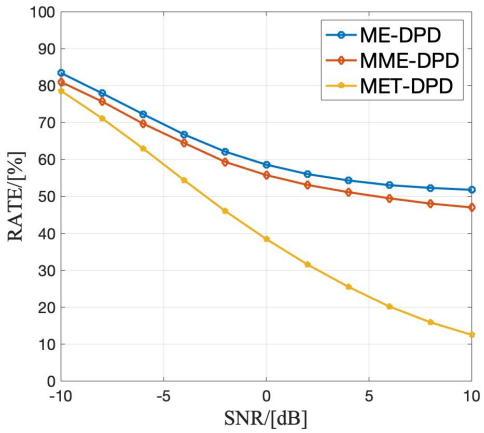

Fig. 6. Difference Rate to Actual Spectrum

Define $\boldsymbol{e} = [\boldsymbol{b}, \boldsymbol{u}]^T$. The formulation (19) can be rewritten as

$$\text{FIM} = \begin{bmatrix} \boldsymbol{J}_{\boldsymbol{r}^o\boldsymbol{r}^o} & \boldsymbol{J}_{\boldsymbol{r}^o\boldsymbol{e}} \\ \boldsymbol{J}_{\boldsymbol{e}\boldsymbol{r}^o} & \boldsymbol{J}_{\boldsymbol{e}\boldsymbol{e}} \end{bmatrix} \tag{25}$$

Thus, the FIM of $\boldsymbol{e}$ can be simplified as

$$\text{FIM} = \boldsymbol{J}_{\boldsymbol{e}\boldsymbol{e}} - \boldsymbol{J}_{\boldsymbol{r}^o\boldsymbol{e}}^T \boldsymbol{J}_{\boldsymbol{r}^o\boldsymbol{r}^o}^{-1} \boldsymbol{J}_{\boldsymbol{r}^o\boldsymbol{e}} \tag{26}$$

The CRLB for estimating the emitter position $\boldsymbol{u}$ can be obtained by taking the inverse of the Fisher matrix $\boldsymbol{J}_{\boldsymbol{\zeta}}^{-1}$ and extracting its lower-right 2×2 submatrix. The above derivation is also applicable to three-dimensional scenarios by extracting its lower-right 3×3 submatrix.

5 Simulation

In this section, simulations are conducted to validate the effectiveness of MET-DPD method.

The distribution of sensor networks and emitter is shown in Fig. 2. The emitter is located at $\boldsymbol{u}_0 = (-50, 0)$m. M=5 sensors are deployed and the initial positions (m) and velocity (m/s) are $\boldsymbol{p}_1 = (1500, -1000)$, $\boldsymbol{p}_2 = (-1000, 1000)$, $\boldsymbol{p}_3 = (10, 1200)$, $\boldsymbol{p}_4 = (1200, 1000)$, $\boldsymbol{p}_5 = (-1500, -1200)$ and $\boldsymbol{v}_1 = (5, -5)$, $\boldsymbol{v}_2 = (0, -6)$, $\boldsymbol{v}_3 = (-5, 5)$, $\boldsymbol{v}_4 = (4, 0)$, $\boldsymbol{v}_5 = (5, 2)$. The emitter signal is linear frequency modulated (LFM) pulse signal, with the bandwidth $B_w = 3$MHz, sampling rate $f_s = 50$MHz and carrier frequency $f_0 = 1$GHz. The number of pulses is 10 and the duration of each pulse is $T = 100\mu$s.

Several DPD methods are simulated to prove the effectiveness of proposed MET-DPD. The first method, ME-DPD, is the traditional DPD method based on the maximum eigenvalue [2,3]. The

second method is refined DPD method based on the ratio of maximum eigenvalue and minimum eigenvalue [11], named MME-DPD. The third one is the proposed MET-DPD method.

The cost function spectrum of the DPD methods with SNR=-10dB, 0dB, 10dB are shown in Fig. 3, Fig. 4, Fig. 5. Compared with ME-DPD and MME-DPD, the proposed MET-DPD can form sharper spectral peaks in the area of interest, thus providing higher-quality preprocessed image data for subsequent multi-source information fusion. To quantify the performance, the difference rate to the actual spectrum is calculated; this metric represents the discrepancy between the cost-function spectrum and the actual spectrum. Note that the actual spectrum is defined as having a value of 1 at position $\boldsymbol{u}_0$ and 0 elsewhere. As shown in Fig. 6, the proposed MET-DPD can bring a significant improvement in the quality of preprocessed image data by utilizing more eigenvalue decomposition information.

6 Conclusion

To accommodate future large-scale sensor network technology, this paper proposes a refined MET-DPD method to obtain the localization cost function spectrum. Passive localization in sensor networks has attracted sustained attention because it can support electromagnetic situational awareness, target monitoring, and cooperative sensing without requiring active signal transmission. In practical environments, however, weak intercepted signals, background noise, and the increasing density of electronic devices make it difficult for conventional methods to generate a clear spectrum for reliable downstream analysis. Against this background, improving the quality of the localization spectrum is meaningful not only for position estimation itself, but also for subsequent information fusion and scene understanding.

By more fully leveraging the eigen-decomposition information, including the maximum eigenvalue and matrix trace, of intercepted signals, the proposed MET-DPD method produces a sharper and more discriminative cost-function spectrum than existing DPD variants. The simulation results demonstrate that the method can better highlight the true emitter position and suppress irrelevant responses over the search region. As a result, it provides higher-quality preprocessed image-like data for subsequent multi-source fusion with optical, infrared, and other sensing modalities. These characteristics make the proposed approach a useful complement to future intelligent sensing systems based on large-scale heterogeneous sensor networks.

Acknowledgments

This work was supported in part by the National Natural Science Foundation of China (No. 62101563).

References

[1] M. Sun and K. C. Ho, “An asymptotically efficient estimator for TDOA and FDOA positioning of multiple disjoint emitters in the presence of sensor location uncertainties,” IEEE Trans. Signal Process. USA, vol. 59, no. 7, pp. 3434-3440, July 2011.

[2] A. J. Weiss and A. Amar, “Direct geolocation of stationary wideband radio signal based on time delays and doppler shifts,” 2009 IEEE/SP 15th Workshop on Statistical Signal Process. Cardiff, UK, pp. 101-104, August 2009.

[3] A. J. Weiss, “Direct position determination of narrowband radio frequency transmitters,” IEEE Signal Process. Lett. USA, vol. 11, no. 5, pp. 513-516, May 2004.

[4] S. Xu, L. Wu, K. Doğançay, M. R. Bhavani Shankar, K. C. Ho and X. Wu, “Optimal sensor placement for target localization in IoT systems: a Cramér-Rao bound perspective,” IEEE Internet Things M. USA, vol. 8, no. 5, pp. 120-126, September 2025.

[5] R. W. Liu, Y. Guo, J. Nie, Q. Hu, Z. Xiong and H. Yu, “Intelligent edge-enabled efficient multi-source data fusion for autonomous surface vehicles in maritime internet of things,” IEEE Trans. Green Commun. Netw. USA, vol. 6, no. 3, pp. 1574-1587, September 2022.

[6] Y. Zhang, G. Wu, X. Li, T. Xu, M. Zhang and F. Guo, “Direct position determination based on passive synthetic aperture for coherent receivers,” IEEE Sens. J. USA, vol. 24, no. 11, pp. 17917-17925, June 2024.

[7] F. Ma, Z. M. Liu and F. Guo, “Direct position determination for wideband sources using fast approximation,” IEEE Trans. Veh. Technol. USA, vol. 68, no. 8, pp. 8216-8221, August 2019.

[8] M. Pourhomayoun and M. L. Fowler, “Sensor network distributed computation for Direct Position Determination,” 2012 IEEE 7th Sensor Array and Multichannel Signal Processing Workshop (SAM), Hoboken, NJ, USA, pp. 125-128, July 2012.

[9] S. He, Y. Jiang and L. Zhao, “Fast direct position determination for moving targets based on PSO,” IEEE Wirel. Commun. Lett. USA, vol. 14, no. 8, pp. 2346-2350, August 2025.

[10] P. Paglierani, “High performance computing and network function virtualization: a major challenge towards network programmability,” 2015 IEEE International Black Sea Conference on Communications and Networking, Constanta, Romania, pp. 137-141, August 2015.

[11] L. Zhao, W. Pu, R. Zhou, M. Y. You and Q. Shi, “Contextual Direct Position Determination for Path Loss Informed Localization,” IEEE Signal Process Lett. USA, vol. 32, pp. 1241-1245, March 2025.